water

MDPI

Article

The Improved Reservoir Module of SWAT Model with a Dispatch Function and Its Application on Assessing the Impact of Climate Change and Human Activities on Runoff Change

Sheng Sheng [1], Qihui Chen [2], Jingjing Li [1] and Hua Chen [1,*]

1 State Key Laboratory of Water Resources Engineering and Management, Wuhan University, Wuhan 430072, China; shengsheng@whu.edu.cn (S.S.); li_jingjing@whu.edu.cn (J.L.)
2 China City Environment Protection Engineering Limited Company, Wuhan 430072, China; qihui_chen@whu.edu.cn
* Correspondence: chua@whu.edu.cn

Abstract: Climate change and human activities significantly impact the hydrological cycle, particularly in regions with numerous large-scale reservoirs. Recognizing the limitations of the reservoir module in the original SWAT model, this study presents an improved reservoir module based on a dispatch function to enhance runoff simulation. Its performance is validated by simulating daily runoff in the Jinsha River Basin, China. The scenario simulation approach is employed to quantitatively analyze the influences of climate change and human activities on runoff. And downscaled Global Climate Models (GCMs) are utilized to predict runoff for the next three decades. The results show that (1) the improved SWAT model outperforms the original model in runoff simulation; (2) during the test period, reservoir regulations caused a reduction of 26 m^3/s in basin outlet runoff, while climate change led to an increase of 272 m^3/s; and (3) future changes in basin outlet runoff over the next 30 years exhibit a high level of uncertainty, ranging from −5.6% to +11.0% compared to the base period. This study provides valuable insights into the hydrological impacts of climate change and human activities, highlighting the importance of incorporating an improved reservoir module in hydrological modeling for more accurate predictions and assessments.

Keywords: SWAT model; climate change; human activities; reservoir operation; attribution analysis

check for updates

Citation: Sheng, S.; Chen, Q.; Li, J.; Chen, H. The Improved Reservoir Module of SWAT Model with a Dispatch Function and Its Application on Assessing the Impact of Climate Change and Human Activities on Runoff Change. *Water* **2023**, *15*, 2620. https://doi.org/10.3390/w15142620

Academic Editors: Xuchun Ye and Chuanzhe Li

Received: 16 June 2023
Revised: 14 July 2023
Accepted: 18 July 2023
Published: 19 July 2023

1. Introduction

As a vital component of the watershed water cycle, runoff plays a crucial role in maintaining the balance of water supply and demand, as well as regulating water quantity [1]. However, the uncertainty surrounding runoff has intensified due to the dynamic nature of the changing environment, posing a primary global concern. A comprehensive understanding of runoff changes and the underlying driving forces is essential for the sustainable utilization and conservation of water resources [2].

It is widely recognized that climate change and human activities constitute two critical factors of the changing environment that influence variations in runoff [3]. Climate change encompasses long-term changes in the Earth's climate system, including temperature, precipitation, wind speed, and humidity [4]. Its impact on runoff can be summarized in two key ways. Firstly, climate change can disrupt precipitation patterns, leading to increased runoff in regions experiencing more frequent or intense rainfall events, while causing decreased runoff in areas facing droughts and reduced precipitation [5]. Secondly, rising temperatures can intensify evaporation, resulting in higher moisture loss and reduced runoff, while also accelerating the melting of ice and snow, contributing to increased runoff in polar regions and certain cold regions [6]. Human activities have diverse impacts on runoff changes, with hydraulic engineering playing a pivotal role. Hydraulic engineering comprises various activities, such as the construction of reservoirs, dams, and irrigation systems [7]. These interventions can significantly alter flow patterns, regulate water allocation, and modify water supply methods, thereby influencing the hydrological processes and runoff within a watershed [8]. Additionally, human activities related to land-use changes, water withdrawal, soil erosion, and pollution also contribute to the modification of the volume and temporal characteristics of runoff [9]. Overall, the combined effects of these human activities and hydraulic engineering practices have a profound influence on the patterns and characteristics of runoff in a given area.

The interaction between climate change and human activities has a combined effect on runoff changes [10]. Climate change, on the one hand, contributes to the intensification of human activities. Meteorological disasters like droughts and floods have prompted the construction of reservoirs and dams, and regional climate disparities between wet and dry areas have led to inter-basin water transfer projects [11]. On the other hand, human activities, such as large-scale afforestation, land enclosure, and reservoir construction, modify the land surface and consequently impact regional climate characteristics [12]. Moreover, human emissions of greenhouse gases have accelerated global warming, further exacerbating climate change impacts. According to the Fifth Assessment Report of the United Nations Intergovernmental Panel on Climate Change (IPCC), human activities are "highly likely" to have been the primary cause of global warming since the mid-20th century, with a probability exceeding 95% [13]. Consequently, understanding and quantifying these impacts of climate change and human activities on runoff are crucial for sustainable water resource management and planning.

Numerous methods have been developed to quantify the impacts of hydrological variables on changes in runoff, which can be classified into four categories: statistical methods, the paired catchment method [14], the field investigation method, and hydrological simulation methods. Among these methods, the statistical analysis method lacks consideration of watershed spatial heterogeneity and hydrological-physical processes. The paired catchment method requires a long test period, incurs high costs, and faces challenges in selecting similar test catchments [15]. The field investigation method relies on detailed data on human activities to calculate naturalized runoff [16]. On the other hand, the hydrological simulation method, based on simulating physical processes using conceptual hydrological models, offers clear physical concepts and high accuracy [17]. It is the most effective tool for studying hydrological response mechanisms. This method assesses the relative contributions of climate change and human activities by comparing observed and simulated runoff during periods of human activities and climate change using calibrated parameters from the baseline period [18].

When conducting a study using the hydrological simulation method to quantify the effect on runoff changes, it is crucial to consider the influence of reservoirs to improve the accuracy of the runoff simulation results. Reservoirs alter the river morphology, flow velocity distribution, and downstream water levels, leading to changes in the spatial and temporal variations of river flow. However, incorporating reservoir regulation in the simulation process poses challenges due to the complexity of reservoir operations. Some scholars have carried out research on this topic, which mainly involves integrating reservoir variables or implementing reservoir algorithms into hydrological models to enable reservoir simulation. Zhao et al. [19] incorporated a multipurpose reservoir module with predefined complex operational rules into the Distributed Hydrology Soil Vegetation Model (DHSVM) and tested the model performance in the upper Brazos River Basin in Texas, where two U.S. Army Corps of Engineers-managed reservoirs are located. The results suggested that the reservoir module holds promise for use in sub-monthly hydrological simulations. Koch et al. [20] integrated the Soil and Water Integrated Model (SWIM) with a reservoir model that represents the storage–release processes based on three management options, including optimized hydropower production, irrigation intake from the reservoir, and optimized provisioning downstream, and found it to be highly flexible when simulating reservoir regulation schemes using a daily time step. Men et al. [21] constructed a reservoir calculation module based on the Hydroinformatic Modeling System (HIMS) model according to the actual situations of the reservoir, and they verified the feasibility of its application to simulate the daily runoff in a reservoir operation period. While hydrological models such as the Soil and Water Assessment Tool (SWAT [22]), The Hydrologic Modeling System (HEC-HMS [23]), and the Large Area Runoff Simulation Model (LARSIM [24]) include modules to consider water withdrawal and reservoir management effects, these modules typically utilize simple tank models. However, these simplified models may not adequately capture the intricacies of more complex reservoir management rules and operations [25]. In the case of the SWAT, the original reservoir module is too simplistic for large-scale comprehensive utilization reservoirs, resulting in poor runoff simulation performance. To address this limitation, this study proposes the use of a dispatch function method based on operation rules to enhance the reservoir module in the SWAT.

The objectives of this study are threefold: (1) to enhance and evaluate the reservoir module in the SWAT, (2) to quantitatively assess the impacts of climate change and human activities on runoff, and (3) to predict future changes in runoff over a 30-year period. The Jinsha River, located in the upper reaches of the Yangtze River in China, is selected as the study area to validate the performance of the proposed SWAT model with dispatch function. It also serves as a representative case study to assess the impact of climate change and reservoir regulation on runoff. The structure of this paper is as follows: Section 2 provides an overview of the study area and data sources. Section 3 presents the methodology used in this study, followed by the presentation of results and the discussion in Sections 4 and 5. Finally, Section 6 presents the conclusions drawn from the study.

2. Study Area and Data

2.1. Study Area

Jinsha River, located in the upper reaches of the Yangtze River, originates from the Tanggula mountains in the eastern part of the Qinghai Tibet Plateau. The Jinsha River Basin covers an area of 455,000 km^2 and experiences annual average precipitation of 631 mm. The basin has an average runoff of 4457 m^3/s and an average temperature of 6.9 °C. Due to the influence of the monsoon climate and the vast coverage of the basin, there are significant spatial and temporal variations in the distribution of meteorological and hydrological elements. The main factors contributing to the basin's runoff are precipitation and the melting of glacier snow. Figure 1 illustrates the geographical position, topography, and hydrological stations in the Jinsha River Basin. Panzhihua, Xiaodeshi, and Pingshan are three main outlet control stations in the Jinsha River Basin. Among them, Xiaodeshi hydrological station is the outlet control station of the Yalong River, the largest tributary of the Jinsha River. Panzhihua station is the control station of the middle reaches of the Jinsha River, and Pingshan station is the general outlet control station of the Jinsha River Basin.

The Jinsha River Basin is renowned for its abundant water resources and vast reserves of water energy. It is home to the Jinsha River and Yalong River hydropower bases, with the Jinsha River Basin hydropower base being the largest in China. Spanning a total length of 3479 km and featuring a natural drop of 5100 m, the Jinsha River contributes to 95% of the total drop along the main stem of the Yangtze River. The reservoirs in the basin serve multiple purposes such as flood control, water supply, power generation, and navigation. These reservoirs have a significant impact on the runoff within the Jinsha River Basin. Currently, there are 13 operational reservoirs along the main course of the Jinsha River and its Yalong River tributaries. Among them, seven reservoirs with notable regulation capabilities were selected for this study, and their specific information is provided in Table 1.

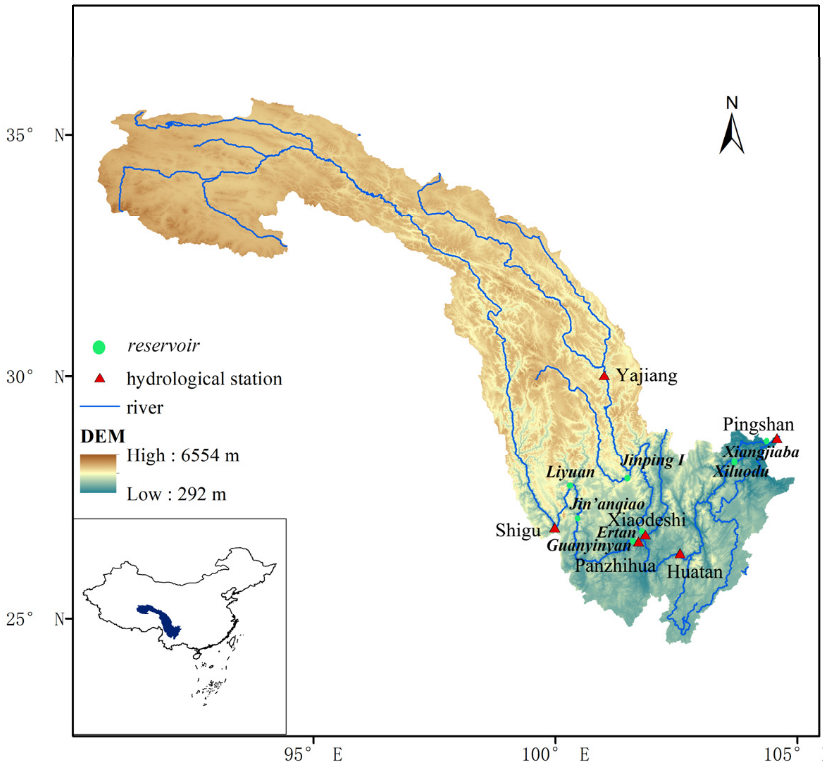

Figure 1. The distribution of reservoirs and hydrological stations in the Jinsha River Basin.

Table 1. Reservoirs with regulation performance above a week in the Jinsha River Basin.

River System	Reservoir	Initial Water Storage Time	Normal Storage Water Level (m)	Regulation Performance	Total Reservoir Capacity (10^8 m^3)
Middle reaches of the Jinsha River	Liyuan	2014.11	1618	weekly	8.05
	Jin'anqiao	2010.11	1418	weekly	9.13
	Guanyinyan	2014.10	1134	weekly	20.72
Lower reaches of the Jinsha River	Xiluodu	2013.5	600	incomplete annual	126.7
	Xiangjiaba	2012.10	380	seasonal	51.63
Lower reaches of the Yalong River	Jinping I	2012.11	1880	annual	77.6
	Ertan	1998.5	1200	seasonal	58

Human activities that impact hydrological processes in the Jinsha River Basin primarily involve changes in land surface and the operation of hydraulic engineering. In our previous study [26], it was found that during the historical period, there were minimal changes in Land Use/Land Cover (LULC) in the Jinsha River Basin, and the influence of LULC change on runoff in this region was deemed insignificant. However, it is important to note that the basin is characterized by numerous large reservoirs, and the effect of reservoir regulation on river runoff cannot be overlooked. Therefore, the impacts of these reservoir projects should be considered when exploring the effects of climate change and human activities on water resources.

2.2. Data

The details of the data utilized in this study are listed in Table 2. The SWAT model is driven by various data sources, including the Digital Elevation Model (DEM), land use, soil data, reservoir operation data, meteorological data, and runoff data. To predict future runoff, meteorological data simulated using different General Circulation Models (GCMs) in the Coupled Model Intercomparison Project Phase 5 (CMIP5) is used.

Table 2. Details of research data.

Datatype	Data Description	Source
DEM	The resolution of 200 m	Geospatial Data Cloud (http://www.gscloud.cn, accessed on 1 May 2020)
Soil data	Harmonized World Soil Database (v1.1), with a resolution of 1000 m	Cold and Arid Regions Sciences Data Center at Lanzhou (http://westdc.westgis.ac.cn, accessed on 1 June 2020)
Land-use data	Land-use dates of 1980, 1990, 2000, 2015, with the resolution of 1000 m	Resources and Environment Data Cloud Platform (http://www.resdc.cn, accessed on 1 June 2020)
Meteorological data	Daily precipitation, min/max/average temperature, relative humidity, solar radiation, and wind speed from 30 weather stations in 1970–2018	China Meteorological Science Data Center (http://data.cma.cn, accessed on 1 July 2020)
Runoff data	Daily runoff data in 6 hydrological stations in 1970–2018	Bureau of Hydrology, Changjiang Water Resources Commission
Reservoir operation data	The storage capacity, daily inflow, outflow, and water level of 7 reservoirs	
GCMs in CMIP5	Daily precipitation, min/max/ The average temperature in 1970–2050	Lawrence Livermore National Laboratory (https://esgf-node.llnl.gov, accessed on 1 July 2020)

3. Methods

This study focuses on improving the reservoir module of the SWAT model and investigating the influence of climate change and human activities on runoff variations based on the improved model. Figure 2 presents the main components employed in this study: the improved SWAT model that incorporates a dispatch function to consider the impact of reservoir operations (Figure 2a); the attribution analysis of the impact of reservoir regulation and climate change on runoff using the scenario simulation method and the improved SWAT model (Figure 2b); and runoff change prediction based on the improved SWAT model under climate change in the next 30 years (Figure 2c).

3.1. The Improved SWAT Model with the Dispatch Function

3.1.1. SWAT Model

The Soil and Water Assessment Tool (SWAT) is a physically based, semi-distributed hydrologic model developed by the United States Department of Agriculture's Agricultural Research Service in the 1980s to simulate long-term changes in hydrologic elements under different land-use types, soil types, and land management practices in large and complex watersheds. It has been widely used all over the world and has proven to behave well in runoff simulation [27,28]. The SWAT can simulate a wide range of physical processes in a watershed, including climate dynamics, hydrological processes, land-cover dynamics, plant growth, erosion and sediment transport, nutrient cycling, and reservoir evolution.

The SWAT model provides four algorithms for calculating reservoir outflow [29]; the outflow is set as (1) the observed daily outflow; (2) the observed monthly outflow; (3) the average annual discharge without control reservoirs; and (4) the function of target capacity for the control reservoir. The first two algorithms require observed outflow files from the reservoir and are not applicable for outflow simulation. The third method is only suitable for free overflow reservoirs that are not artificially regulated. Only the target reservoir capacity method can be used for the outflow simulation of reservoirs in the Jinsha River Basin, but its applicability is limited to large integrated reservoirs with functions of flood control, water supply, power generation, navigation, etc.

The hydrological parameters of the SWAT model are calibrated using the Uncertainty in Sequential Uncertainty Fitting (SUFI-2) optimization algorithm [30,31] based on data from before the initial water storage time of the first large-scale reservoir in the Jinsha River Basin. Specifically, the calibration period spans from 1985 to 1997, which has relatively complete hydrometeorological data, while the validation period covers 1970 to 1984, which has less complete data.

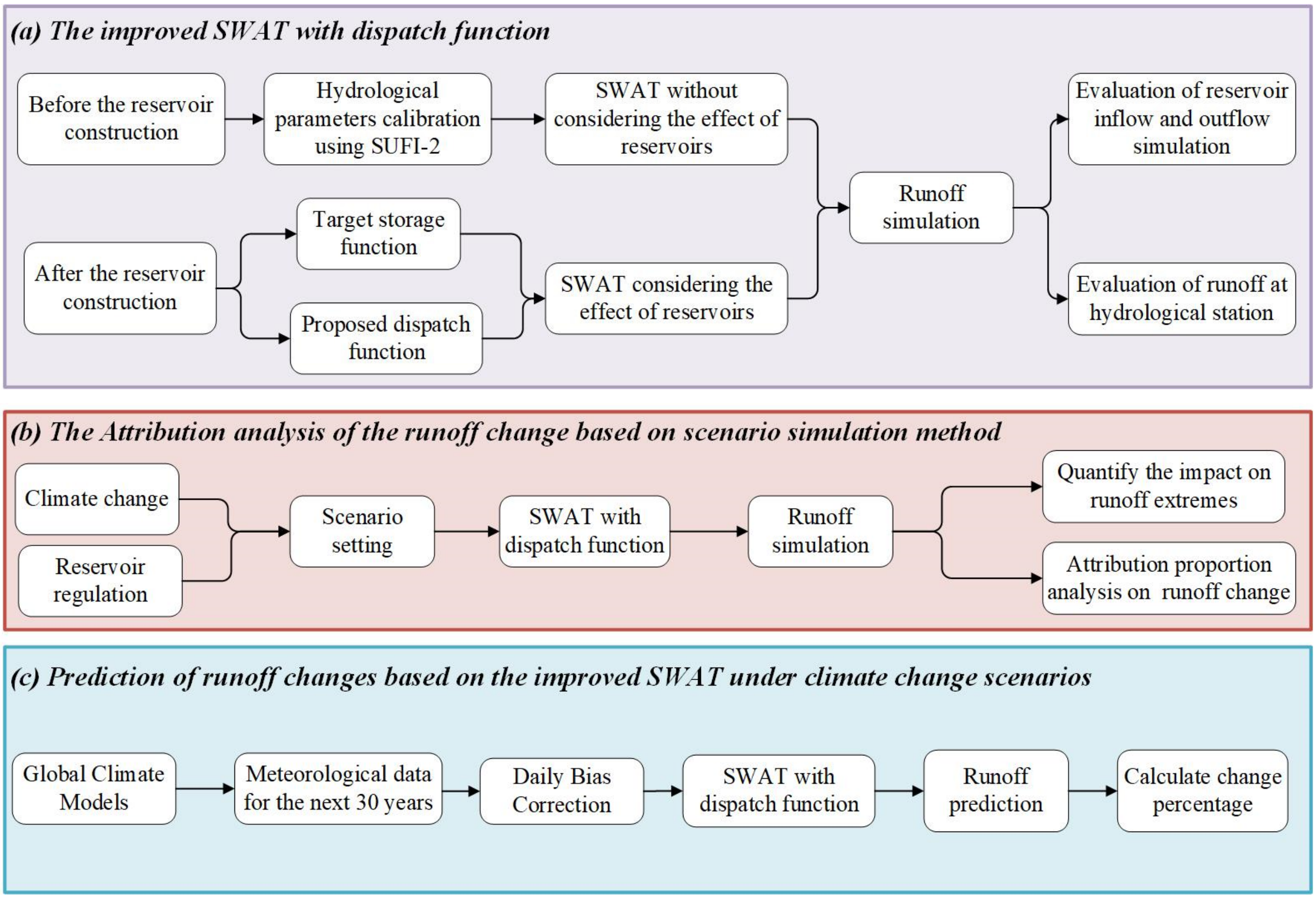

Figure 2. Main architectures adopted in this study.

3.1.2. The Dispatch Function

In this study, a dispatch function method is chosen to improve the reservoir module in the SWAT model, aiming for simplicity and ease of implementation. The dispatch function utilizes the reservoir inflow of the current period I_t and the reservoir outflow of the previous period Q_{t-1} as independent variables. The reservoir outflow of the current period Q_t is treated as the dependent variable, and a binary linear regression model is used to establish the dispatch function (Equation (1)). To ensure the reliability of the regression analysis, the three sigma rule [32,33] is applied to eliminate any regression outliers. According to this rule, data points that fall outside the range of three standard deviations from the mean are considered abnormal or outliers. The resulting reservoir outflow calculation function is then incorporated into the SWAT model as the new and improved reservoir module.

$$Q_t = \alpha_1 I_t + \alpha_2 Q_{t-1} + c \quad (1)$$

where Q_{t-1} and Q_t are reservoir outflow of the last moment and this moment, respectively. I_t is the reservoir inflow at this moment; α_1 and α_2 are the regression coefficients of the corresponding independent variables. c is the constant.

In addition to the dispatch function, this study also incorporates some reservoir operation constraints to prevent computational dispersion leading to increased simulation errors. These constraints ensure that the reservoir operates within defined parameters and responds appropriately to different water storage levels. Under normal circumstances, the outflow R_t should fall within the following range:

$$Q_{\min} \leq Q_t \leq Q_{\max} \quad V_d \leq V_t \leq V_f \tag{2}$$

where $Q_{\min}$ and $Q_{\max}$ are the minimal and maximal values of historical observed outflow; V_t denotes the water storage at t-th period; and V_d and V_f represent the dead storage and flood storage of the reservoir.

In certain exceptional scenarios, the outflow is determined based on the water storage at this period:

$$Q_t = \begin{cases} V_t - V_f, & V_t > V_f \\ Q_{\min}, & \frac{V_d}{2} \leq V_t < V_d \\ 0, & V_t < \frac{V_d}{2} \end{cases} \tag{3}$$

3.1.3. Evaluation Indicators

The performance of the SWAT model is evaluated using three indicators, including the Nash–Sutcliffe efficiency (NSE) [34], the coefficient of determination (R^2), and percent bias ($PBIAS$) [35]. NSE and R^2 reflect the matching degrees of the data series. The closer they are to 1, the better the simulation result is. The $PBIAS$ reflects the simulation deviation of the mean runoff value. The closer it is to 0, the better the simulation result is. They are calculated as follows:

$$NSE = 1 - \frac{\sum_{i=1}^{n} (Q_{obs,i} - Q_{sim,i})^2}{\sum_{i=1}^{n} (Q_{obs,i} - \overline{Q_{obs}})^2} \tag{4}$$

$$R^2 = \frac{\left[\sum_{i=1}^{n} (Q_{obs,i} - \overline{Q_{obs}})(Q_{sim,i} - \overline{Q_{sim}})\right]^2}{\sum_{i=1}^{n} (Q_{obs,i} - \overline{Q_{obs}})^2 \sum_{i=1}^{n} (Q_{sim,i} - \overline{Q_{sim}})^2} \tag{5}$$

$$PBIAS = \left(1 - \frac{\sum_{i=1}^{n} Q_{sim,i}}{\sum_{i=1}^{n} Q_{obs,i}}\right) \times 100\% \tag{6}$$

where n is the total number of days; $Q_{obs,i}$ and $Q_{sim,i}$ are the observed and simulated runoff, respectively; and $\overline{Q_{obs}}$ and $\overline{Q_{sim}}$ are the mean values of observed and simulated runoff series, respectively.

3.2. Attribution Analysis of the Impact of Reservoir Regulation and Climate Change on Runoff

3.2.1. Mann–Kendall Trend Test

Mann–Kendall trend test is a non-parametric statistical test used to assess the presence and significance of trends in time series data [36,37]. It uses a two-tailed test, and under a given significance level α, if $|Z| > Z_{1-\alpha/2}$, it is considered to have a significant trend in the series; otherwise, it is considered to have no significant trend [38]. $|Z|$ reflects the strength of the trend in the series. Additionally, a positive Z value indicates an upward trend, while a negative Z value indicates a downward trend. In this study, a significance level of $\alpha = 0.05$ is chosen, corresponding to $Z_{1-\alpha/2} = \pm 1.96$, to test the trend in the series.

3.2.2. Scenario Setting and Simulation Method

The scenario simulation method [26,39] is adopted to distinguish the impacts of climate change and reservoir regulation on runoff. Considering the operation of large-scale reservoirs and the available meteorological and hydrological data, the historical period from 1970 to 2018 is divided into two equal-length periods: the reference period (P_{ref}, 1970–1989) and the test period (P_{test}, 1999–2018). Four scenarios are formulated by combining the climate data and reservoir operating conditions of P_{ref} and P_{test} (Table 3), and the runoff for each scenario is simulated using the improved SWAT model with the dispatch function.

Table 3. The setting of 4 scenarios.

Scenarios	Reservoir Regulation	Climate Data	Mean Annual Simulated Runoff Depth (mm)
S1	P_{ref}	P_{ref}	R_1 (benchmark)
S2	P_{test}	P_{ref}	R_2 (only influenced by reservoirs)
S3	P_{ref}	P_{test}	R_3 (only influenced by climate)
S4	P_{test}	P_{test}	R_4 (jointly influence)

Scenario S1 uses the climate data and reservoir operating conditions during the P_{ref} period, and its mean annual simulated runoff depth R_1 is used as the benchmark for the other three scenarios. Scenario S2 uses the climate data during the P_{ref} and the reservoir operating conditions in the P_{test}; therefore, R_2 represents mean annual simulated runoff depth under the impact of reservoir regulation. Scenario S3 uses the climate data of the P_{test} with the reservoir operating conditions during the P_{ref}, and R_3 represents the mean annual simulated runoff depth under the impact of climate change. Scenario S4 uses climate data and the reservoir operating conditions during the P_{test} to drive the SWAT model, and R_4 represents the mean annual simulated runoff depth under the combined impacts of climate change and reservoir regulation.

3.2.3. Quantitative Assessment of the Impact on Runoff

Four indicators of extreme runoff values (annual maximum 1-day, 5-day, 15-day runoff and the 95th percentile of daily runoff series) are selected to quantify the impact of climate change and reservoir regulation on runoff extremes. The rate of influence (IR_i) of different influencing factors on the runoff extreme values can be calculated as follows:

$$IR_i = \frac{R_{i\_\max} - R_{1\_\max}}{R_{1\_\max}} \times 100\% \tag{7}$$

where $R_{1\_\max}$ and $R_{i\_\max}$ represent the extreme values of simulated runoff extreme values under different scenarios.

The contributions of climate change and reservoir regulation to runoff variations can be calculated as follows:

$$P'_{res} = \frac{R_2 - R_1}{R_4 - R_1} \times 100\% \tag{8}$$

$$P'_{cc} = \frac{R_3 - R_1}{R_4 - R_1} \times 100\% \tag{9}$$

where P'_{cc} and P'_{res} (%) are the relative contribution ratios of climate change and reservoir regulation on runoff. To make the attribution proportions of the two factors add up to 100%, the attribution proportions are redistributed to P_{res} and P_{cc}:

$$P_{res} = \frac{P'_{res}}{P'_{res} + P'_{CC}} \tag{10}$$

$$P_{cc} = \frac{P'_{cc}}{P'_{res} + P'_{cc}} \tag{11}$$

where P_{cc} and P_{res} (%) are the attribution proportions of climate change and reservoir regulation on runoff.

3.3. Runoff Change Prediction under Climate Change in the Next 30 Years

3.3.1. Selection of Typical GCMs

To predict the runoff in Jinsha River Basin in the future, the meteorological data of GCMs are used to drive the SWAT. Many GCMs are participating in CMIP5. A total of 25 and 28 GCMs under RCP4.5 and RCP8.5 emission scenarios are used in this study. In order to reduce the complexity of simulation results and avoid information redundancy, typical GCMs are selected based on 10% and 90% quantiles of changes in precipitation and temperature [40]. The results are listed in Table S1. Under RCP8.5, the GCM corresponding to the typical cold-dry and warm-dry climate scenarios is the same. Therefore, a total of 7 typical GCMs under the two emission scenarios are selected for future hydrological prediction. GCMs are downscaled using the Daily Bias Correction (DBC) downscaling methods [41].

3.3.2. Runoff Prediction under Climate Change

Based on the corrected precipitation and temperature data from seven selected GCMs, the improved SWAT model with the dispatch function is used to predict runoff for the next 30 years (2023–2050). The study designates the period from 1970 to 2005 as the base period and defines three forecasting periods: 2023–2030, 2031–2040, and 2041–2050. The change percentage of the predicted runoff under different forecasting periods with respect to the base period (1970–2005) is calculated using the following formula:

$$D = \frac{\overline{R}_{forecast} - \overline{R}_{base}}{\overline{R}_{base}} \times 100\% \tag{12}$$

where D is the change percentage and $\overline{R}_{forecast}$ and $\overline{R}_{base}$ represent the average annual runoff volumes for the forecasting and base periods.

4. Results

In this section, a comparison is made between the daily runoff simulated by the improved reservoir model and the original SWAT model (Section 4.1). The impacts of climate change and human activities on runoff are quantitatively assessed using the improved model (Section 4.2). Furthermore, a prediction of future runoff in the Jinsha River Basin is presented in Section 4.3.

4.1. The Improved SWAT Model with a Dispatch Function

4.1.1. Hydrological Parameter Calibration before the Reservoir Impact Period

The results of parameter calibration for the SWAT model in simulating daily runoff at the six hydrological stations are presented in Table 4. During both the calibration and validation periods, the R^2 for all stations surpasses 0.8, indicating a strong correlation between the simulated and observed data. Additionally, the *PBIAS* falls within the range of ±15%, indicating a satisfactory agreement between the simulated and observed mean runoff values. Except for the Shigu and Yajiang stations, the *NSE* exceeds 0.8, further confirming the reliable performance of the model. The average values of R^2, *NSE*, and *PBIAS* for the six hydrological stations during the calibration periods are 0.88, 0.85, and 5.63%, respectively. And the average values for the same indicators during the validation periods are 0.88, 0.85, and 7.82%. These calibration results demonstrate the robustness and accuracy of the SWAT model in simulating daily runoff at the hydrological stations in the study area before the reservoir impact period.

Table 4. Parameter calibration result of the SWAT model for simulating daily runoff in Jinsha River Basin.

Stations	Water System	Calibration Period (1985–1997)			Validation Period (1970–1984)		
		R^2	*NSE*	*PBIAS* (%)	R^2	*NSE*	*PBIAS* (%)
Yajiang	Yalong River	0.82	0.80	−3.4	0.80	0.79	3.7
Xiaodeshi	Yalong River	0.88	0.86	13.1	0.86	0.83	14.8
Shigu	Upper Jinsha River	0.82	0.77	10.2	0.83	0.78	12.3
Panzhihua	Middle reaches of Jinsha River	0.89	0.84	−3.5	0.90	0.86	0.7
Huatan	Lower reaches of Jinsha River	0.93	0.92	6.4	0.93	0.92	2.1
Pingshan	Lower reaches of Jinsha River	0.94	0.92	11.0	0.93	0.91	13.3
Absolute average		0.88	0.85	5.63	0.88	0.85	7.82

Figure 3 presents the simulated runoff for the validation period at the Pingshan hydrological station, which serves as the representative outlet of the Jinsha River Basin. Based on the figure, it is evident that the calibrated SWAT model performs satisfactorily in simulating runoff during the validation period unaffected by reservoir operations. The simulated hydrograph closely aligns with the observed hydrograph, indicating a good overall agreement in capturing the general trends of flood fluctuations. However, it is worth noting that the simulated runoff tends to underestimate the flood peak, especially when peak flows exceed 15,000 m^3/s. This substantial discrepancy between the simulated and observed peak values can be attributed to the limited occurrence of extreme large flood events with peak flows exceeding the threshold during the calibration period. It is challenging to adequately calibrate the model parameters to accurately represent extreme flood events. As a consequence, the model's ability to accurately simulate peak flows is slightly compromised, leading to a relatively poorer performance in this aspect.

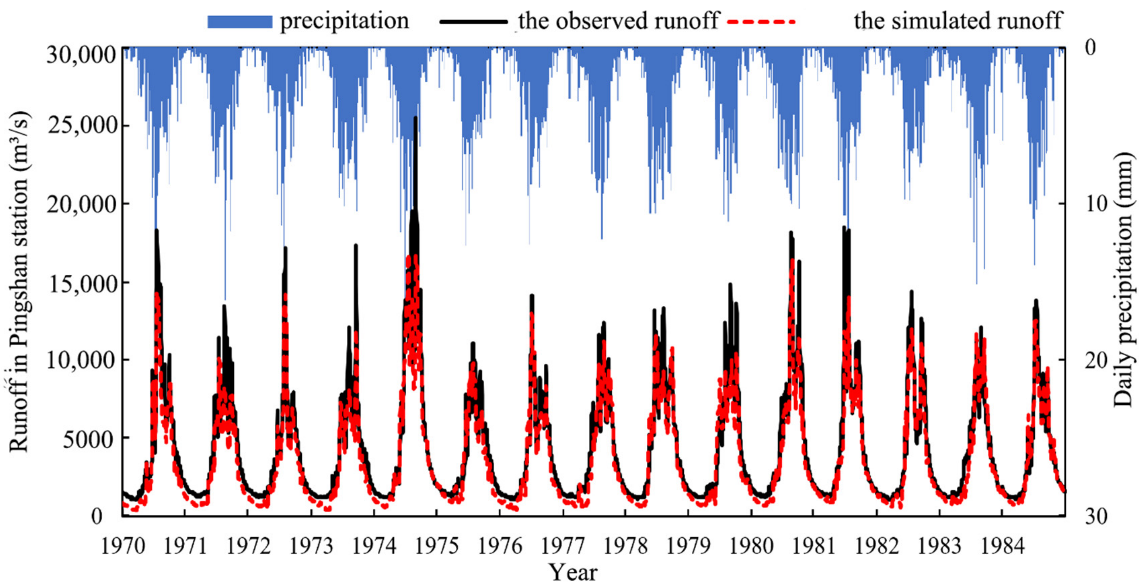

Figure 3. Runoff simulation results of Pingshan station during the validation period.

Considering the results from Figure 3 and Table 4, it can be inferred that the SWAT model performs satisfactorily in simulating runoff in the Jinsha River Basin prior to the construction of reservoirs. The model captures the essential hydrological processes and accurately reproduces the observed runoff patterns. These findings provide confidence in the model's capability to simulate pre-reservoir runoff conditions and serve as a solid foundation for further analysis and investigation related to the impacts of reservoir construction and other factors regarding the basin's hydrological regime.

4.1.2. The Dispatch Function of Reservoirs

Due to substantial variations in reservoir operating rules throughout different periods, this study classifies the reservoir operation period into two distinct seasons: the flood season (May to October) and the non-flood season (November to April of the following year). For each season, specific dispatch functions and correlation coefficients are presented in Table 5. As can be seen from the table, the correlation coefficients for most of the dispatch functions are above 0.9. And for individual reservoirs, the correlation coefficients for the dispatch functions are basically higher in the flood season than in the non-flood season.

Table 5. The dispatch function of reservoirs.

Reservoirs	Flood Season		Non-Flood Season	
	Dispatch Function	**CC**	**Dispatch Function**	**CC**
Ertan	$Q_t = 0.265I_t + 0.732Q_{t-1} - 56.0$	0.94	$Q_t = 0.152I_t + 0.799Q_{t-1} + 54.4$	0.88
Jinping I	$Q_t = 0.136I_t + 0.760Q_{t-1} + 120.6$	0.93	$Q_t = -0.011I_t + 0.969Q_{t-1} + 26.9$	0.97
Liyuan	$Q_t = 0.863I_t + 0.140Q_{t-1} - 3.47$	0.99	$Q_t = 0.465I_t + 0.531Q_{t-1} + 0.67$	0.91
Jin'anqiao	$Q_t = 0.647I_t + 0.357Q_{t-1} - 45.0$	0.98	$Q_t = 0.107I_t + 0.779Q_{t-1} + 45.5$	0.87
Guanyinyan	$Q_t = 0.461I_t + 0.522Q_{t-1} + 42.4$	0.96	$Q_t = 0.153I_t + 0.771Q_{t-1} + 79.4$	0.91
Xiluodu	$Q_t = 0.409I_t + 0.518Q_{t-1} + 212.5$	0.94	$Q_t = 0.066I_t + 0.859Q_{t-1} + 220.8$	0.90
Xiangjiaba	$Q_t = 0.542I_t + 0.374Q_{t-1} + 852.6$	0.97	$Q_t = 0.090I_t + 0.905Q_{t-1} + 79.1$	0.95

The fitting results of the dispatch functions to the reservoir outflow are presented in Table S2. The table indicates that, in general, the regression results during the flood season are better compared to those during the non-flood season. With the exception of the Jin'anqiao Reservoir during the non-flood season, the NSE and R^2 reach 0.8 and above, and the $PBIAS$ is less than ±5%. To investigate the reasons for the relatively poorer simulation results of the Jin'anqiao Reservoir during the non-flood season, the observed and simulated outflows are plotted in Figure S1. The plot reveals great fluctuations in the observed outflow of the Jin'anqiao Reservoir during the non-flood season, which presents challenges for accurate fitting. However, despite these challenges, the simulation results are still considered acceptable. Overall, the dispatch function demonstrates satisfactory performance in simulating reservoir outflow.

4.1.3. Evaluation of the Improved SWAT Based on Reservoir Inflow and Outflow Simulation

The first reservoir on the Jinsha River began to store water in May 1997. Thus, 1998–2018 is selected as the reservoir impact period. The simulated inflow and outflow of reservoirs based on the SWAT with the dispatch function method are compared with those obtained using the SWAT with the target storage function method and the SWAT without considering reservoir influence, and the results are presented in Table S3.

It can be observed that the inflow simulation is consistent among the three methods for the Jinping I reservoir, which can be attributed to the absence of large upstream reservoirs. Additionally, the inflow/outflow simulation results of the SWAT with the dispatch function method are similar to those of the SWAT without considering reservoir influence for the reservoirs in the middle reaches of the Jinsha River, including Liyuan, Jin'anqiao, and Guanyinyan. Both methods outperform the target storage capacity method. These three reservoirs have limited storage capacity and flood-control capability. For the four reservoirs with seasonal regulation ability (Jinping I, Ertan, Xiluodu, and Xiangjiaba), the inflow/outflow simulation results of the SWAT with the dispatch function method are superior to the other methods. This indicates that the suitability of the SWAT with the dispatch function method is better demonstrated in reservoirs with greater regulation ability. Overall, the SWAT model with the dispatch function method exhibits superior performance compared to the SWAT with the target storage capacity method and the SWAT without considering reservoir influence.

Taking Ertan Reservoir as an example, in Figure 4, the outflow simulated using three methods is compared to the observed outflow. From the figure, it can be observed that the dispatch function method performs the best among the three approaches, followed by the method without considering reservoir effects, while the target storage capacity method exhibits the poorest performance. The target storage capacity method exhibits an abnormal pattern in the simulated flow process, where there is a significant increase in outflow on May 1st each year, followed by a sudden drop to zero on November 1st. This anomaly is due to the configuration of the target storage capacity in the method. During the non-flood season, the target storage is set to the spillway capacity without any flood-control reserve, while during the flood season, a certain flood-control capacity is reserved based on the soil moisture content. As a result, there is a sudden change in the target storage capacity of the reservoir on the transition days between the flood season and the non-flood season (1 May and 1 November), leading to a corresponding abrupt change in the outflow. In the SWAT model without considering reservoir effects, the outflow from the reservoir is set equal to the inflow, neglecting the reservoir's regulation. Therefore, during certain simulation scenarios, the simulated peak flow tends to be overestimated, and the timing of the peak occurs earlier than in reality. The dispatch function method, which takes into account the reservoir management rules, performs well in capturing the variations in flood patterns and accurately simulating the peak flow compared to the other two methods.

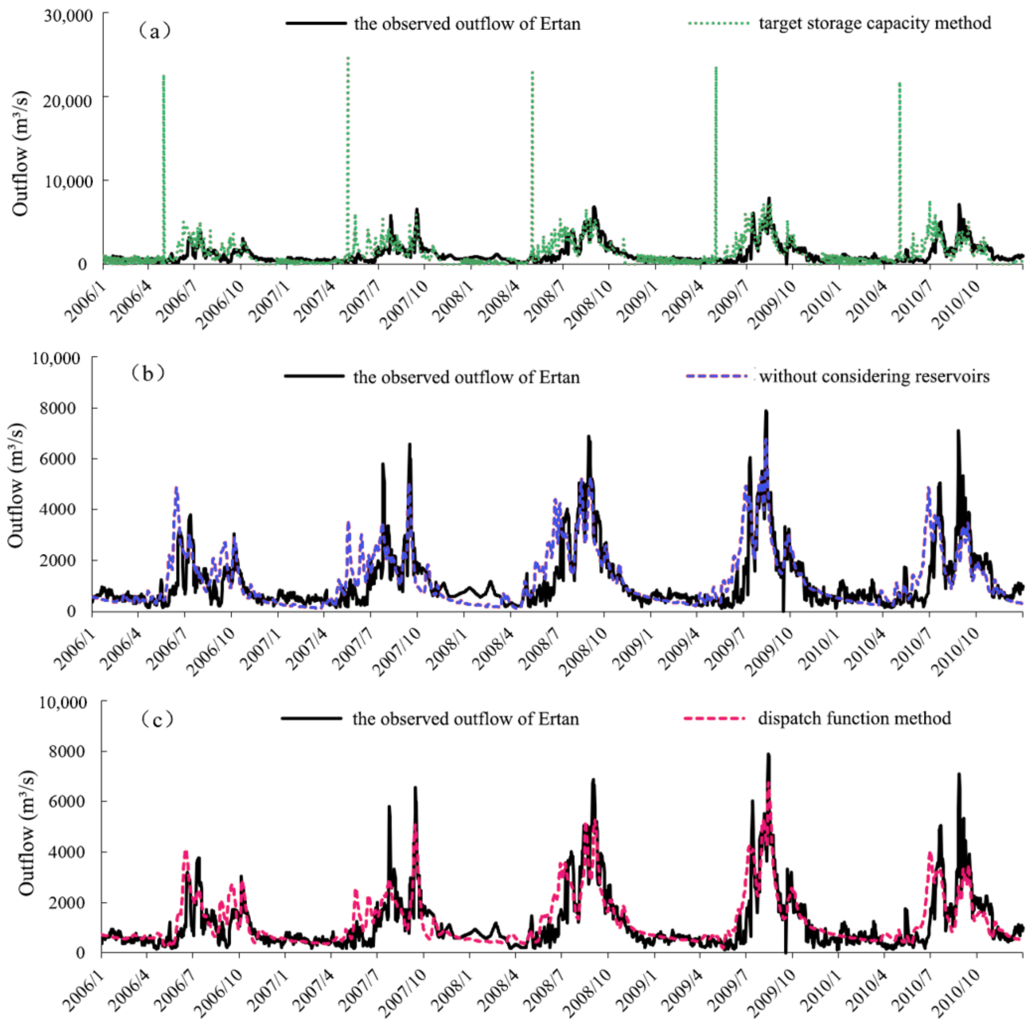

Figure 4. Comparison of observed and SWAT-simulated outflow with three reservoir algorithms at Ertan Reservoir. (**a**) Simulated outflow of SWAT with the target storage capacity method; (**b**) Simulated outflow of SWAT without considering the influence of reservoirs; (**c**) Simulated outflow of SWAT with the dispatch function.

In conclusion, the target storage capacity method in the SWAT is not suitable for the inflow/outflow simulation of large-scale comprehensive utilization reservoirs. Compared with the SWAT without considering reservoir influence and with the target storage capacity method, the SWAT with the dispatch function method has better applicability for reservoirs with strong regulation ability.

4.1.4. Evaluation of the Improved SWAT Based on Runoff Simulation at Hydrological Stations

The runoff processes of six hydrological stations (Yajiang, Xiaodeshi, Shigu, Panzhihua, Huatan, and Pingshan) in the Jinsha River Basin were also simulated during the reservoir impact period. The simulation results obtained using the SWAT with three different reservoir modules are presented in Table 6.

Table 6. Simulation accuracy of hydrological stations with different reservoir algorithms.

Station Evaluation Period		**Yajiang 1998–2008**	**Shigu 2011–2018**	**Xiaodeshi 1999–2018**	**Panzhihua 2011–2018**	**Huatan 2011–2018**	**Pingshan 2011–2018**
Target storage capacity method	*NSE*	0.84	0.77	−0.78	0.69	0.57	0.37
	R^2	0.84	0.86	0.24	0.84	0.73	0.66
	PBIAS (%)	2.6	−10	−3.2	−17.9	−4.2	0.9
Without considering the reservoir influence	*NSE*	0.84	0.77	0.52	0.71	0.75	0.73
	R^2	0.84	0.86	0.58	0.86	0.83	0.82
	PBIAS (%)	2.6	−10	−5.4	−18.4	−5.3	−1.2
Dispatch function method	*NSE*	0.84	0.77	0.67	0.72	0.84	0.78
	R^2	0.84	0.86	0.68	0.85	0.87	0.80
	PBIAS (%)	2.6	−10	−3.1	−17.8	−4.0	1.4

From the table, it can be observed that for the hydrological stations without upstream reservoirs, including Yajiang and Shigu stations, the runoff simulation performs well, and the different reservoir modules do not affect accuracy. For the remaining four hydrological stations influenced by upstream reservoirs (Xiaodeshi, Panzhihua, Huadan, and Pingshan stations), the simulation performance of the target storage capacity method is generally poor, with *NSE* values of −0.78, 0.69, 0.57, and 0.37, respectively. On the other hand, the simulation results of the other two methods are better, especially the dispatch function method. Compared to not considering reservoirs, the dispatch function method increases the *NSE* values by 0.15, 0.09, 0.01, and 0.05 for the four stations, respectively, indicating that it can improve the accuracy of hydrological process simulation in basins affected by reservoirs. The simulation performance of the dispatch function method for the Panzhihua hydrological station is similar to that of not considering reservoirs, possibly due to the relatively small regulating capacity of the Liyuan, Jin'anqiao, and Guanyinyan reservoirs upstream of the Panzhihua station, resulting in weaker regulation of river runoff. Overall, compared to the SWAT with the target storage capacity method and the algorithm that does not consider reservoirs, the SWAT with the dispatch function method demonstrates clear superiority in simulating the runoff process for hydrological stations with significant reservoir disturbances. Therefore, the SWAT with the target storage capacity method will be utilized in the subsequent assessment of the impacts of climate change and human activities on runoff in the Jinsha River Basin.

4.2. Attribution Analysis on Runoff Changes

4.2.1. Trend Analysis of Runoff

The runoff changes during 1970–2018 at six hydrological stations in the basin were counted and plotted as a 5-year sliding average in Figure 5. The red dashed lines in the figure indicate linear trends in runoff changes, and the marked Z values are the Mann–Kendall trend statistics for annual runoff at each hydrological station. Figure 5 shows that in the past 50 years, the annual runoff of Yajiang, Xiaodeshi, Shigu, and Panzhihua stations fluctuated greatly and shows a significant upward trend (Z > 1.96). Those four stations are located in the upper and middle reaches of the Jinsha River and the Yalong River. In contrast, the annual runoff of the Huatan and Pingshan hydrological stations in the lower reaches of the Jinsha River has no significant change trend. Furthermore, the runoff from three hydrological stations in the middle and lower reaches of the Jinsha River (Panzhihua, Huabang, and Pingshan) has shown a more pronounced decline since the 21st century.

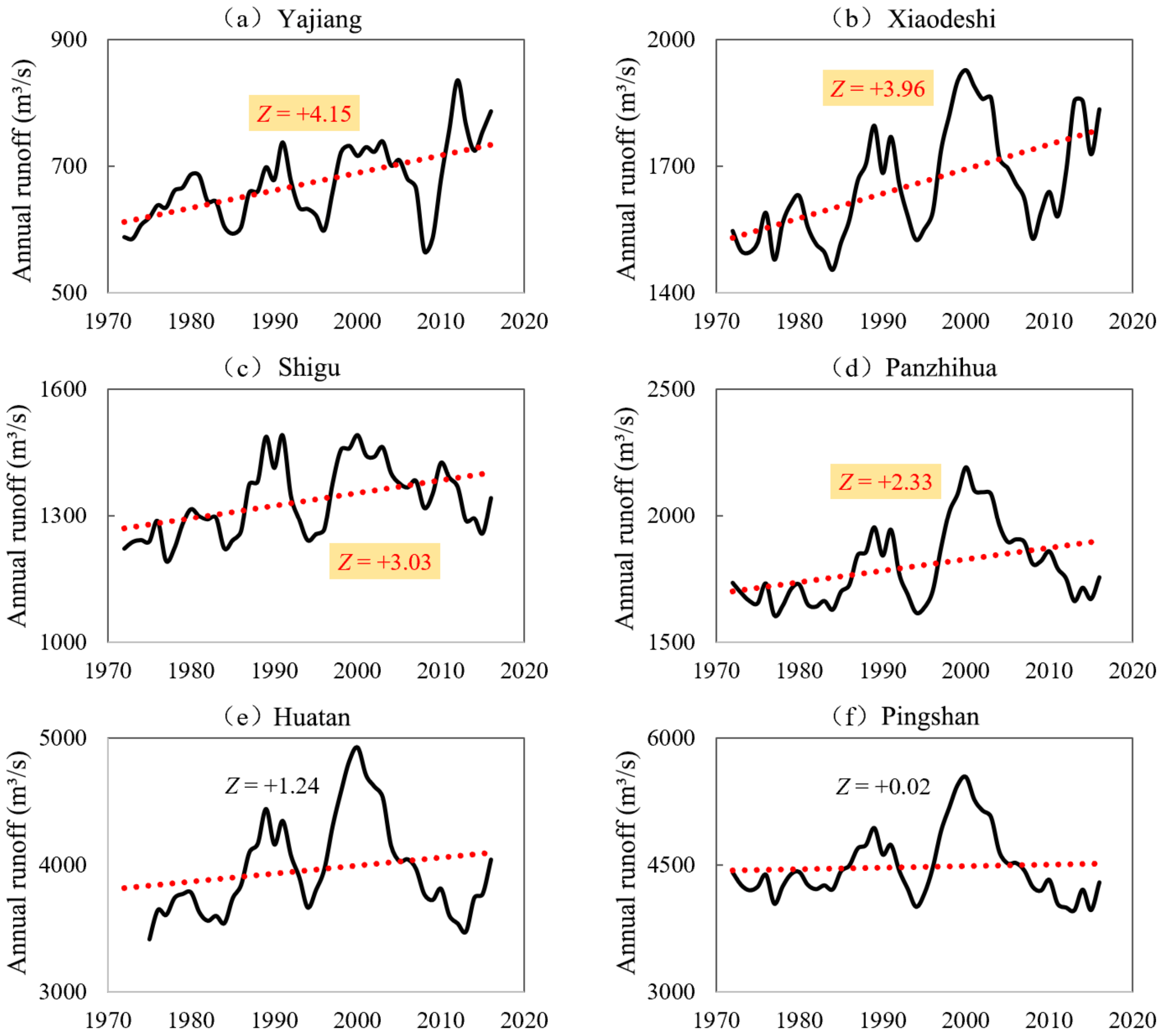

Figure 5. Changes in annual runoff at hydrological stations in the Jinsha River Basin from 1970 to 2018. The black and red lines indicate the runoff changes over years and linear trends, respectively.

The runoff coefficient, defined as the ratio of the volume of runoff to the total volume of precipitation during a certain period, is an important indicator that reflects the characteristics of runoff generation and routing in the river basin. Based on the precipitation and runoff data of the study area in the historical period, the changes in the runoff coefficient of the Jinsha River Basin over the past 50 years were counted, and the results are shown in Figure 6. It shows that the runoff coefficient of the Jinsha River Basin does not show a significant change trend during 1970 and 1999. However, the runoff coefficient dropped from 0.53 to 0.34 from 2000 to 2017, and the rate of decrease was 0.1 per 10 years. The runoff coefficient rebounded to a certain extent in 2018.

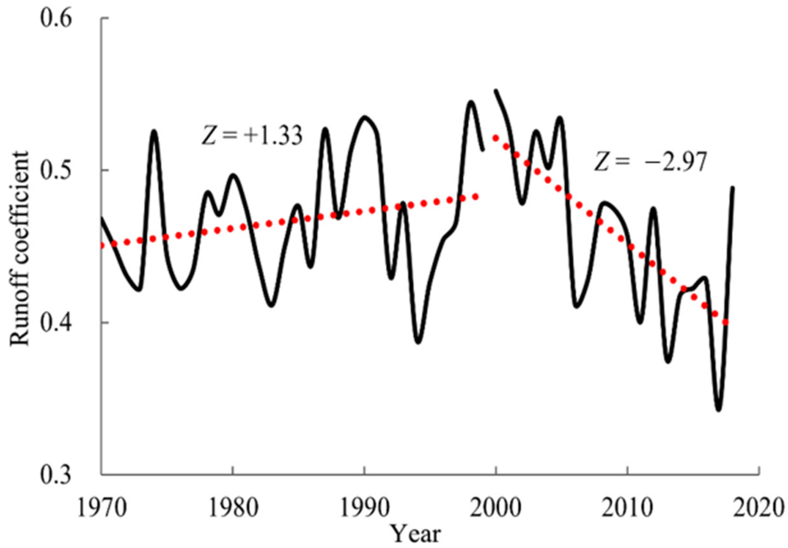

Figure 6. Changes in runoff coefficient in the Jinsha River Basin from 1970 to 2018. The black and line indicates the change of runoff coefficient over years; and the red lines indicate the linear trends of changes in different periods.

4.2.2. Quantitative Assessment of the Impacts of Climate Change and Human Activities on Extreme Runoff

Due to the satisfactory performance of the SWAT model in simulating the maximum runoff values at various hydrological stations within the watershed, four indicators of maximum runoff values (annual maximum 1-day, 5-day, 15-day runoff, and the 95th percentile of daily runoff series) are selected to analyze the daily runoff series at the three major control stations simulated using the SWAT under four scenarios for each station during the P_{ref} to P_{test} period. The average values of the four extreme indicators simulated using the SWAT model under the four scenarios in the Jinsha River Basin are shown in Figure 7. Among them, the simulated values corresponding to Scenario S1 are used as a reference; S2 and S3 represent the impacts of hydraulic engineering and climate change, respectively; and the simulated values under Scenario S4 represent the combined effects of both.

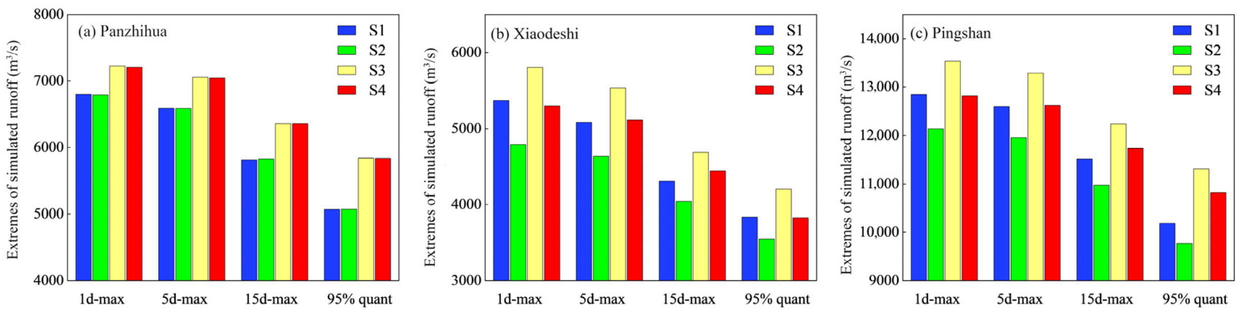

Figure 7. Multi-year averages of runoff extremes for the three main control stations simulated using the SWAT for the S1~S4 scenarios.

It can be seen that for the same station, the variations of the four extreme runoff indicators under different scenarios are similar. This is because all four indicators reflect the maximum values of the runoff series and have a certain positive correlation. For the Panzhihua station, the impact of water conservancy projects on the extreme runoff values is minimal, possibly due to the relatively weak regulation capacity of the upstream reservoirs (as reflected by the reservoir capacity values of various middle reaches of the Jinsha River in Table 1), while climate change causes an increase in all four extreme indicators. The combined effect of the two factors leads to a significant increase in the maximum runoff values at the Panzhihua station. For the Xiaodeshi and Pingshan stations, the operation of hydraulic engineering during the historical period resulted in a significant decrease in the maximum runoff values, while the effect of climate change is the opposite. Under the combined effect of the two factors, there is no apparent direction of change in the maximum runoff values at these two control stations.

To visually demonstrate the impact of hydraulic engineering and climate change on the maximum runoff values during the P_{ref} to P_{test} period, the influence rates of different factors on the maximum runoff are calculated at the three control stations, and the results are shown in Table 7. Negative values indicate that the factor contributes to a decrease in the maximum runoff values, represented in blue, while positive values indicate an increase, represented in red.

Table 7. The influence rates of water conservancy projects and climate change on the maximum runoff values at the three control stations during the P_{test} period (1999–2018) relative to the P_{ref} period (1970–1989).

Influence Rate (%)		Hydraulic Engineering	Climate Change	Joint Effect
Panzhihua	1d-max	−0.1	6.3	6.1
	5d-max	−0.1	7.0	6.9
	15d-max	0.2	9.4	9.4
	95% quant	0.0	15.1	15.1
Xiaodeshi	1d-max	−10.7	8.2	−1.2
	5d-max	−8.9	8.8	0.5
	15d-max	−6.2	8.7	3.1
	95% quant	−7.6	9.6	−0.2
Pingshan	1d-max	−5.4	5.4	−0.2
	5d-max	−5.1	5.5	0.2
	15d-max	−4.7	6.3	1.9
	95% quant	−4.2	11.0	6.2

Notes: Blue and red respectively indicate the negative and positive values of the influence rate. The darker the color, the greater the difference from 0.

According to the table, for the Panzhihua station, the influence rate of water conservancy projects on the maximum runoff values is very low, ranging from −0.1% to +0.2%. In contrast, the influence rate of climate change is significantly larger, ranging from +6.3% to +15.1%. Therefore, climate change dominates the impact on the maximum runoff values at this station, and the combined effect of both factors leads to a noticeable increase in the maximum runoff values. In comparison to the Panzhihua station, the response of the Xiaoheishi and Pingshan stations to hydraulic engineering is more pronounced. The water conservancy projects significantly decrease the maximum runoff values at both hydrological stations, with reduction rates ranging from −10.7% to −6.2% and from −5.4% to −4.2%, respectively. On the other hand, climate change leads to a significant increase in the maximum runoff values, with increases ranging from +8.2% to +9.6% and from +5.4% to +11.0%, respectively. The combined effect of both factors results in minor changes in the maximum runoff values, and there is no consistent direction of change. Comparing the scenario simulation results for the maximum runoff values at the three major control stations, it can be observed that climate change during the historical period has led to a significant increase in the maximum runoff values at all three stations. However, for the Xiaoheishi and Pingshan hydrological stations, the operation of upstream large-scale hydraulic engineering has greatly mitigated the increase in maximum runoff values, reflecting the "peak-shaving" effect of water conservancy projects on river runoff.

4.2.3. Quantitative Assessment of the Impacts of Climate Change and Human Activities on Mean Runoff

Figure 8 shows the mean annual runoff of the three main controlling stations simulated by the SWAT under different scenarios. It can be seen that the simulated runoff of the three stations under the four scenarios changes similarly: compared to scenario S1, the runoff of scenario S2 slightly decreases; the runoff of scenario S3 increases significantly; and the runoff of scenario S4 also increases but is slightly smaller than that of S3. It can be preliminarily judged that from period P_{ref} to P_{test}, reservoir regulation reduced the river runoff in the Jinsha River Basin, while climate change increased the runoff, and its impact was significantly higher than that of reservoir regulation. Under the combined influence of the two, the mean annual runoff of the three main control stations in the Jinsha River Basin has increased a lot.

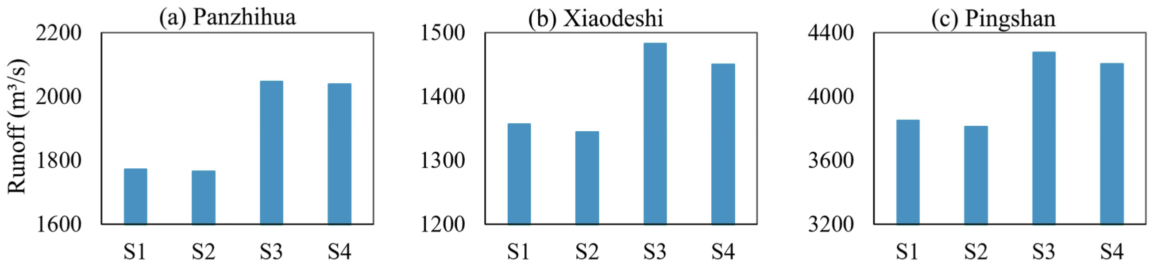

Figure 8. The annual mean runoff of three main control stations simulated by the SWAT under the four scenarios.

The attribution proportions of climate change and reservoir regulation on annual mean runoff are calculated, and the results are shown in Table 8. It can be seen that from period P_{ref} to P_{test}, the attribution proportions of reservoir regulation for Panzhihua, Xiaodeshi, and Pingshan stations are −2.0%, −11.3%, and −10.6%, respectively. The attribution proportions of climate change are +102.0%, +111.3%, and +110.6%, respectively. Taking the outlet station of Pingshan as an example, from the reference period (P_{ref}) to the test period (P_{test}), the measured runoff in the entire basin increased by 246 m^3/s. As part of this, the operation of hydraulic engineering resulted in a decrease of 26 m^3/s in runoff, while climate change led to an increase of 272 m^3/s in runoff. On the one hand, the operation of reservoirs during the P_{test} period has to some extent reduced the runoff in the Jinsha River Basin, with the storage capacity of large reservoirs playing a significant role in intercepting and regulating river runoff. On the other hand, climate change has a positive impact on runoff, mainly due to increased precipitation (the average annual precipitation in the entire basin increased from 616 mm in the P_{ref} period to 645 mm in the P_{test} period). Furthermore, the impact of climate change on runoff is much greater than that of reservoir regulation, indicating that climate change plays a dominant role in influencing river runoff.

Table 8. The attribution proportions of climate change and reservoir regulation on annual mean runoff.

Attribution Proportions (%)	Panzhihua	Xiaodeshi	Pingshan
Reservoir regulation	−2.0	−11.3	−10.6
Climate change	+102.0	+111.3	+110.6

4.3. Prediction of Runoff Changes in Future under Climate Change Scenarios

4.3.1. Changes of Meteorological and Hydrological Elements in Future

The runoff in the Jinsha River Basin for the next 30 years is simulated using the improved SWAT with the dispatch function using meteorological data from typical GCMs. The changes in meteorological and hydrological elements are shown in Figure 9. Compared with the base period, the annual precipitation and temperature predicted using the seven typical GCMs increased by +0.7%~+11.0% (equivalent to +4.5 mm~+69.3 mm/year) and +1.0 °C~+2.1 °C, respectively. There is no consistent direction of change in runoff. Three GCMs predict that the runoff in the next 30 years will decrease compared with the base period, and the other four GCMs predict that the runoff will increase. In general, the runoff of the Jinsha River Basin in the next 30 years will vary from −5.6% to +11.0% compared with the base period (equivalent to the annual runoff increase of −16.9 mm to +33.1 mm). It indicates that although precipitation is the primary factor influencing basin runoff, other factors, including temperature, also have an impact on runoff. Therefore, an increase in precipitation does not necessarily lead to a consistent change in runoff.

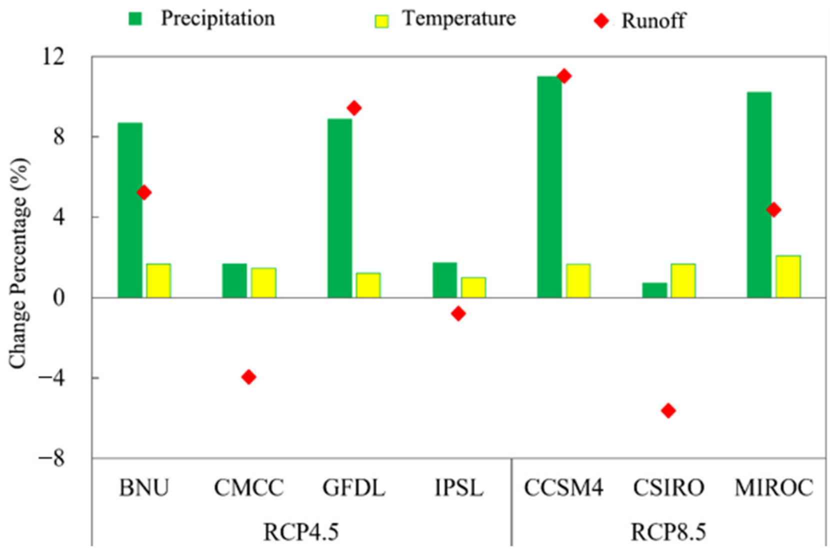

Figure 9. The changes in precipitation, temperature, and runoff in the Jinsha River Basin in the next 30 years (2021–2050) compared with the base period (1970–2005).

4.3.2. Change Percentages of Simulated Runoff under Different Decades

Based on the predicted runoff in different forecast periods, the change percentage compared with the base period (1970–2005) is calculated according to Equation (10), and the results are presented in Figure 10. It plots the change percentage of simulated runoff under different forecast periods compared with the base period (1970–2005) of six hydrological stations. Figure 10 shows that the runoff of Yajiang and Xiaodeshi hydrological stations, which are located in the middle and lower reaches of the Yalong River, has no noticeable change in direction in the next 30 years. The variation in runoff simulated by different typical GCMs varies significantly, and there is a large uncertainty in their runoff variability. For Shigu and Panzhihua hydrological stations in the middle reaches of Jinsha River, the runoff predicted by most typical GCMs in the next 30 years increases compared to the base period, and only the runoff predicted by RCP4.5-CMCC and RCP8.5-CSIRO is slightly decreased. Therefore, it can be presumed with a high degree of confidence that the runoff at the Shigu and Panzhihua hydrological stations will increase to a certain extent in the next 30 years compared to the base period, especially in the years 2023–2030 and 2041–2050 when the upward trend is more obvious. Due to the close hydraulic connection between the two hydrological stations of the lower Jinsha River, the predicted changes in runoff from different typical GCMs are relatively similar. In general, there is no consistent direction of change in runoff at the Huabang and Pingshan stations across the forecasting periods, except for the more obvious positive change in runoff predicted by different GCMs from 2041 to 2050, indicating that there is greater uncertainty in the change of runoff in the lower Jinsha River over the next 30 years, and no more reliable evolutionary characteristics can be predicted for the time being.

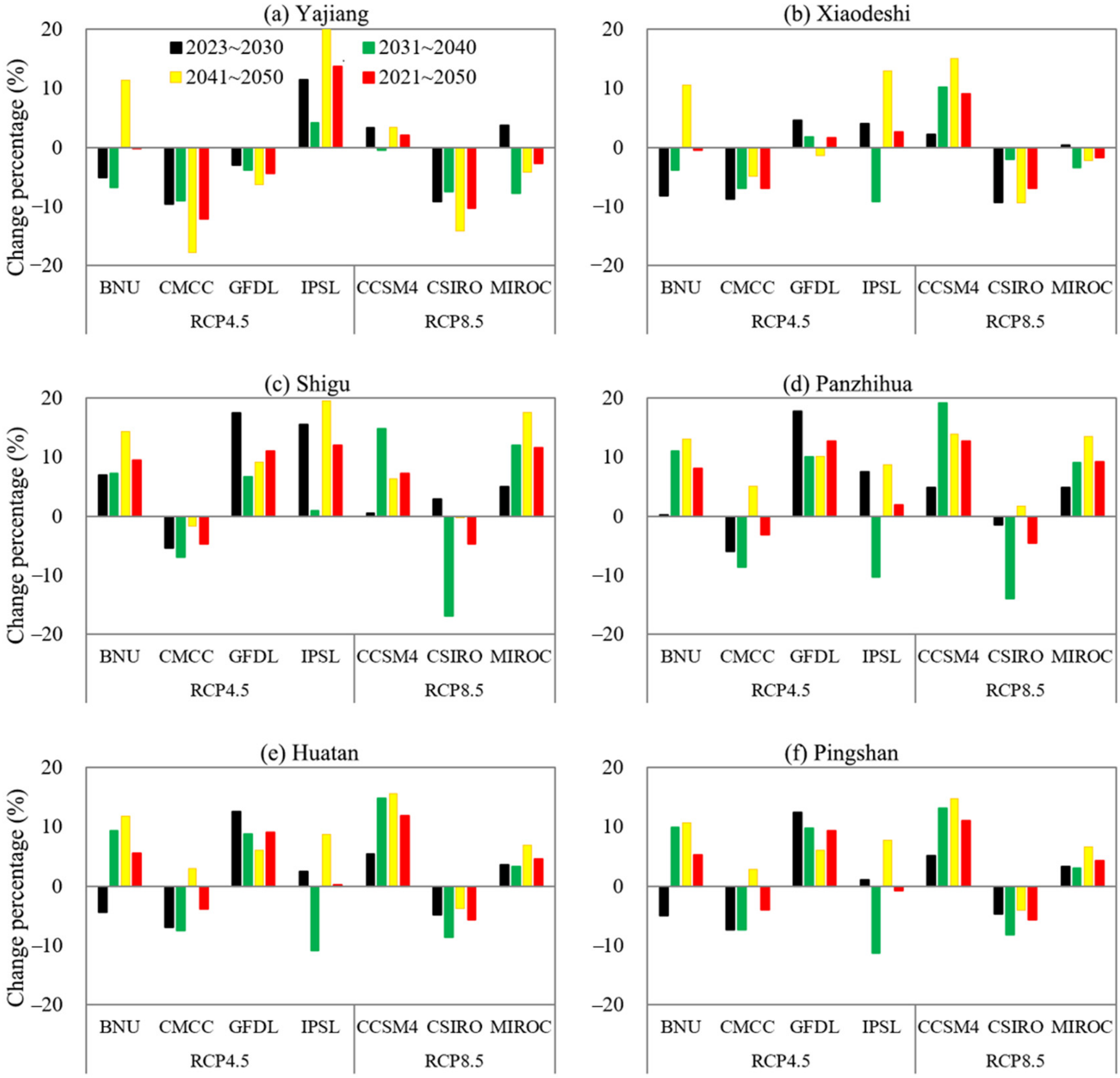

Figure 10. The change percentage of simulated runoff of six hydrological stations under different forecast periods compared with the base period (1970–2005).

Additionally, for Pingshan station, the main station of Jinsha River, the growth rate of the runoff in the cold-wet climate scenario (RCP4.5-GFDL and RCP8.5-CCSM4) is the largest, followed by that in the warm-wet climate scenario (RCP4.5-BNU and RCP8.5-MIROC). The growth rate in warm-dry climate scenarios (RCP4.5-CMCC and RCP8.5-CSIRO) is the smallest. The results show that the order of the predicted runoff change rate under different typical climate scenarios is as follows: cold-wet > warm-wet > cold-dry > warm-dry. It is consistent with the positive correlation between precipitation and runoff and the negative correlation between temperature and runoff. Meanwhile, it shows that precipitation influences the runoff change more than temperature.

5. Discussion

The original reservoir module in the SWAT model has limitations in its applicability, particularly the widely used target storage capacity method, which is not suitable for large-scale multipurpose reservoirs. To address this issue, this study proposes a dispatch function-based reservoir module and integrates it into the SWAT model to enhance its performance. The effectiveness of this method is evaluated through daily runoff simulations at reservoirs and hydrological stations. In the proposed reservoir module (Equation (1)), the inflow from the current period and the outflow from the previous period are selected as independent variables, while the outflow from the current period is considered the dependent variable. By applying a binary linear regression model, the dispatch function for major regulation reservoirs is derived separately for the flood season and non-flood season. The correlation coefficients are generally above 0.9, with higher goodness of fit observed during the flood season (Table 5), indicating the reliability of the dispatch function as a basis for reservoir outflow calculations within the SWAT model. The dispatch function takes into account the regulating function of large-scale multipurpose reservoirs and provides a better simulation of reservoir outflow. It outperforms the target storage capacity method and the SWAT that neglects reservoir influence in terms of result validity and accuracy (Figure 4). Using the improved SWAT model for runoff simulation, it is found that the enhanced model greatly improves the accuracy of runoff simulation, especially for hydrological stations influenced by large upstream reservoirs with strong regulation capabilities (Table 6).

Based on the previous research findings [26,42,43], climate change and reservoir regulation are identified as two main influencing factors. Using scenario simulation methods and the improved SWAT model, this study quantitatively analyzes the impacts of these two factors on the mean and extreme values of runoff. Attribution analysis conducted on the changes in runoff extremes (Table 7) reveals that for stations with weak upstream reservoir regulation, the influence of the reservoir is minimal, and climate change dominates the variability of extreme values at these locations. However, in the presence of large-scale regulating reservoirs upstream, their operation mitigates the increase in extreme runoff values caused by climate change, showcasing the peak-shaving effect of water engineering on river runoff [44]; therefore, no clear directional change in maximum runoff values is observed. Furthermore, attribution analysis of mean runoff changes (Table 8) indicates that large reservoirs have a storage effect on river runoff, reducing the long-term average runoff in the basin to some extent [45,46]. On the other hand, climate change has a positive impact on runoff, and its influence far exceeds that of reservoirs [47]. Consequently, the combined effect of both factors leads to a significant increase in the long-term average runoff in the basin.

Based on data from seven representative GCMs under the RCP4.5 and RCP8.5 emission scenarios, it is observed that both precipitation and temperature exhibit an increasing trend over the next 30 years, with precipitation showing a larger rate of change compared to temperature in most cases (Figure 9). Utilizing the meteorological data from these GCMs, the improved SWAT model is employed to simulate runoff for the next 30 years. The results reveal significant uncertainty in runoff changes, with no clear direction of change observed (Figure 10). While precipitation is identified as the primary factor influencing runoff, an increase in precipitation does not necessarily result in a consistent change in the direction of runoff due to the influence of other elements. Future research could explore the interactions between precipitation, temperature, and other climate variables to gain a deeper understanding of their impacts on runoff patterns and improve predictions in the face of climate change.

6. Conclusions

The operation of reservoirs significantly impacts the pattern of runoff and poses challenges for simulating watershed runoff. To address the limitations of the original reservoir module in the SWAT model, a dispatch function method is proposed in this study and is integrated with the SWAT model to improve runoff simulation. The model's performance is validated through simulating daily runoff in the Jinsha River Basin in China. Based on the improved SWAT model, the quantitative assessment of the impacts of climate change and human activities on runoff is conducted through scenario simulations. Additionally, the runoff changes in the next 30 years under climate change are predicted by incorporating the meteorological data of seven typical GCMs from CMIP5. The conclusions are as follows:

(1) The dispatch function method exhibits superior performance in simulating reservoir outflow and runoff at hydrological stations compared to the original reservoir module in the SWAT model. The advantages of the dispatch function method are more pronounced when applied to reservoirs with greater regulation capacity.
(2) The attribution analyses demonstrate that the operation of reservoirs leads to a certain reduction in the basin's runoff volume. However, the positive impact of climate change on runoff is more pronounced and has a dominant effect on river runoff.
(3) Over the next 30 years, both precipitation and temperature will increase compared to the base period (1970–2005), with a larger increase in precipitation. However, the changes in runoff do not follow a consistent pattern and exhibit a higher level of uncertainty. An increase in precipitation does not necessarily result in a proportional change in runoff.

The findings provide valuable insights for water resource management and decision-making in the face of changing environmental conditions. It is worth noting that the proposed dispatch function method has limitations in practical applications. It relies on historical operational data of the reservoir, limiting its applicability to reservoirs with a history of stable operations. In future research, it is recommended to collect and study technical documents, such as reservoir operation charts or scheduling regulations, to overcome these limitations and improve the accuracy and applicability of reservoir outflow simulation.

Supplementary Materials: The following supporting information can be downloaded at: https://www.mdpi.com/article/10.3390/w15142620/s1, Figure S1: Outflow of Jin'anqiao Reservoir simulated by linear regression in non-flood season (2016–2017); Table S1: Typical GCMs under two RCPs and their spatial resolution; Table S2: Results of fitting the reservoir outflow based on dispatch function; Table S3: Simulation accuracy of different reservoir algorithms for inflow and outflow of seven reservoirs in the Jinsha River Basin.

Author Contributions: Conceptualization, S.S. and Q.C.; methodology, S.S. and Q.C.; software, S.S. and Q.C.; validation, S.S. and J.L.; formal analysis, S.S. and Q.C.; data curation, J.L.; writing—original draft preparation, S.S.; writing—review and editing, J.L. and H.C.; supervision, H.C.; funding acquisition, H.C. All authors have read and agreed to the published version of the manuscript.

Funding: This research was funded by the National Key Research and Development Program (2022YFC3002701).

Data Availability Statement: The runoff data and reservoir operation data provided by the Bureau of Hydrology, Changjiang Water Resources Commission are not publicly available. The rest of the research data are publicly available datasets downloaded from the internet and accessed as described in Section 2.2.

Conflicts of Interest: The authors declare no conflict of interest.

Nomenclature

Abbreviations	**Full Name**
BNU	Beijing Normal University Earth System Model
CCSM4	Community Climate System Model version 4
CMCC	Cambiamenti Climatici Climate Model
CMIP5	Coupled Model Intercomparison Project Phase 5
CSIRO	Commonwealth Scientific and Industrial Research Organisation
DEM	Digital Elevation Model
DHSVM	Distributed Hydrology Soil Vegetation Model
GCM	Global Climate Model
GFDL	Geophysical Fluid Dynamics Laboratory
HEC-HMS	Hydrologic Engineering Center-Hydrologic Modeling System
HIMS	Hydroinformatic Modeling System
IPCC	Intergovernmental Panel on Climate Change

Abbreviations	Full Name
IPSL	Institute Pierre Simon Laplace
LARSIM	Large Area Runoff Simulation Model
LULC	Land Use/Land Cover
MIROC	Model for Interdisciplinary Research on Climate
P_{ref}	Reference period
P_{test}	Test period
RCP	Representative Concentration Pathway
SUFI-2	Uncertainty in Sequential Uncertainty Fitting
SWAT	Soil and Water Assessment Tool
SWIM	Soil and Water Integrated Model

References

1. Dey, P.; Mishra, A. Separating the impacts of climate change and human activities on streamflow: A review of methodologies and critical assumptions. *J. Hydrol.* **2017**, *548*, 278–290. [CrossRef]
2. Xu, Y.; Wang, S.; Bai, X.; Shu, D.; Tian, Y. Runoff response to climate change and human activities in a typical karst watershed, SW China. *PLoS ONE* **2018**, *13*, e0193073. [CrossRef] [PubMed]
3. Zhang, Y.; Wang, M.; Chen, J.; Zhong, P.-A.; Wu, X.; Wu, S. Multiscale attribution analysis for assessing effects of changing environment on runoff: Case study of the Upstream Yangtze River in China. *J. Water Clim. Chang.* **2020**, *12*, 627–646. [CrossRef]
4. Di Cicco, M.E.; Ferrante, G.; Amato, D.; Capizzi, A.; De Pieri, C.; Ferraro, V.A.; Furno, M.; Tranchino, V.; La Grutta, S. Climate Change and Childhood Respiratory Health: A Call to Action for Paediatricians. *Int. J. Environ. Res. Public Health* **2020**, *17*, 5344. [CrossRef] [PubMed]
5. Zeng, F.; Ma, M.-G.; Di, D.-R.; Shi, W.-Y. Separating the Impacts of Climate Change and Human Activities on Runoff: A Review of Method and Application. *Water* **2020**, *12*, 2201. [CrossRef]
6. McCrystall, M.R.; Stroeve, J.; Serreze, M.; Forbes, B.C.; Screen, J.A. New climate models reveal faster and larger increases in Arctic precipitation than previously projected. *Nat. Commun.* **2021**, *12*, 6765. [CrossRef] [PubMed]
7. Wang, J.; Xue, L.; Zhou, L.; Wei, L.; Hu, S.; Wu, H.; Zhang, H.; Xiang, C.; Li, X. Cumulative ecosystem response to Hydraulic Engineering Infrastructure Projects in an arid basin. *Sci. Total Environ.* **2023**, *856*, 159110. [CrossRef]
8. Ai, P.; Xiong, C.; Li, K.; Song, Y.; Gong, S.; Yue, Z. Effect of Data Characteristics Inconsistency on Medium and Long-Term Runoff Forecasting by Machine Learning. *IEEE Access* **2023**, *11*, 11601–11612. [CrossRef]
9. Wu, L.; Zhang, X.; Hao, F.; Wu, Y.; Li, C.; Xu, Y. Evaluating the contributions of climate change and human activities to runoff in typical semi-arid area, China. *J. Hydrol.* **2020**, *590*, 125555. [CrossRef]
10. Omer, A.; Wang, W.; Basheer, A.K.; Yong, B. Integrated assessment of the impacts of climate variability and anthropogenic activities on river runoff: A case study in the Hutuo River Basin, China. *Hydrol. Res.* **2016**, *48*, 416–430. [CrossRef]
11. Tien Bui, D.; Talebpour Asl, D.; Ghanavati, E.; Al-Ansari, N.; Khezri, S.; Chapi, K.; Amini, A.; Thai Pham, B. Effects of Inter-Basin Water Transfer on Water Flow Condition of Destination Basin. *Sustainability* **2020**, *12*, 338. [CrossRef]
12. Cheng, G.; Liu, Y.; Chen, Y.; Gao, W. Spatiotemporal variation and hotspots of climate change in the Yangtze River Watershed during 1958–2017. *J. Geogr. Sci.* **2022**, *32*, 141–155. [CrossRef]
13. de Larminat, P. Earth climate identification vs. anthropic global warming attribution. *Annu. Rev. Control* **2016**, *42*, 114–125. [CrossRef]
14. Van Loon, A.F.; Rangecroft, S.; Coxon, G.; Breña Naranjo, J.A.; Van Ogtrop, F.; Van Lanen, H.A.J. Using paired catchments to quantify the human influence on hydrological droughts. *Hydrol. Earth Syst. Sci.* **2019**, *23*, 1725–1739. [CrossRef]
15. Shahid, M.; Cong, Z.; Zhang, D. Understanding the impacts of climate change and human activities on streamflow: A case study of the Soan River basin, Pakistan. *Theor. Appl. Climatol.* **2018**, *134*, 205–219. [CrossRef]
16. Zhang, A.; Zhang, C.; Fu, G.; Wang, B.; Bao, Z.; Zheng, H. Assessments of Impacts of Climate Change and Human Activities on Runoff with SWAT for the Huifa River Basin, Northeast China. *Water Resour. Manag.* **2012**, *26*, 2199–2217. [CrossRef]
17. Zhan, C.S.; Jiang, S.S.; Sun, F.B.; Jia, Y.W.; Niu, C.W.; Yue, W.F. Quantitative contribution of climate change and human activities to runoff changes in the Wei River basin, China. *Hydrol. Earth Syst. Sci.* **2014**, *18*, 3069–3077. [CrossRef]
18. Li, Z.; Huang, S.; Liu, D.; Leng, G.; Zhou, S.; Huang, Q. Assessing the effects of climate change and human activities on runoff variations from a seasonal perspective. *Stoch. Environ. Res. Risk Assess.* **2020**, *34*, 575–592. [CrossRef]
19. Zhao, G.; Gao, H.; Naz, B.S.; Kao, S.-C.; Voisin, N. Integrating a reservoir regulation scheme into a spatially distributed hydrological model. *Adv. Water Resour.* **2016**, *98*, 16–31. [CrossRef]
20. Koch, H.; Liersch, S.; de Azevedo, J.R.G.; Silva, A.L.C.; Hattermann, F.F. Assessment of observed and simulated low flow indices for a highly managed river basin. *Hydrol. Res.* **2018**, *49*, 1831–1846. [CrossRef]
21. Men, B.; Liu, H.; Tian, W.; Wu, Z.; Hui, J. The Impact of Reservoirs on Runoff Under Climate Change: A Case of Nierji Reservoir in China. *Water* **2019**, *11*, 1005. [CrossRef]
22. Dash, S.S.; Sahoo, B.; Raghuwanshi, N.S. How reliable are the evapotranspiration estimates by Soil and Water Assessment Tool (SWAT) and Variable Infiltration Capacity (VIC) models for catchment-scale drought assessment and irrigation planning? *J. Hydrol.* **2021**, *592*, 125838. [CrossRef]

23. Naqash, T.B.; Ahanger, M.A.; Maity, R. Multi-site hydrometeorological simulation of streamflow for upper Jhelum basin in northwest Himalayas using HEC–HMS soil moisture accounting algorithm. *Model. Earth Syst. Environ.* **2023**, *9*, 431–455. [CrossRef]
24. Ishikawa, M.; Haag, I.; Krumm, J.; Teltscher, K.; Lorke, A. The effect of stream shading on the inflow characteristics in a downstream reservoir. *River Res. Appl.* **2021**, *37*, 943–954. [CrossRef]
25. Koch, H.; Liersch, S.; Hattermann, F.F. Integrating water resources management in eco-hydrological modelling. *Water Sci. Technol.* **2013**, *67*, 1525–1533. [CrossRef]
26. Chen, Q.; Chen, H.; Zhang, J.; Hou, Y.; Shen, M.; Chen, J.; Xu, C. Impacts of climate change and LULC change on runoff in the Jinsha River Basin. *J. Geogr. Sci.* **2020**, *30*, 85–102. [CrossRef]
27. Cao, Y.; Zhang, J.; Yang, M.; Lei, X.; Guo, B.; Yang, L.; Zeng, Z.; Qu, J. Application of SWAT Model with CMADS Data to Estimate Hydrological Elements and Parameter Uncertainty Based on SUFI-2 Algorithm in the Lijiang River Basin, China. *Water* **2018**, *10*, 742. [CrossRef]
28. Yuan, S.; Quiring, S.M.; Kalcic, M.M.; Apostel, A.M.; Evenson, G.R.; Kujawa, H.A. Optimizing climate model selection for hydrological modeling: A case study in the Maumee River basin using the SWAT. *J. Hydrol.* **2020**, *588*, 125064. [CrossRef]
29. Neitsch, S.; Arnold, J.; Kiniry, J.; Williams, J. *Soil and Water Assessment Tool Theoretical Documentation, Version 2009, Texas Water Resources Institute Technical Report No.406*; Texas Water Resources Institute: Texas, TX, USA, 2011.
30. Abbaspour, K.C.; Yang, J.; Maximov, I.; Siber, R.; Bogner, K.; Mieleitner, J.; Zobrist, J.; Srinivasan, R. Modelling hydrology and water quality in the pre-alpine/alpine Thur watershed using SWAT. *J. Hydrol.-Amst.* **2007**, *333*, 413–430. [CrossRef]
31. Abbaspour, K.C.; Johnson, C.A.; Genuchten, M. Estimating Uncertain Flow and Transport Parameters Using a Sequential Uncertainty Fitting Procedure. *Vadose Zone J.* **2004**, *3*, 1340–1352. [CrossRef]
32. Pukelsheim, F. The Three Sigma Rule. *Am. Stat.* **1994**, *48*, 88–91. [CrossRef]
33. Xiao, H.; Zhang, Y.; Liu, X.; Yin, H.; Liu, P.; Liu, D.C. A Rapid Ultrasound Vascular Disease Screening Method using PauTa Criterion. *J. Phys. Conf. Ser.* **2021**, *1769*, 012009. [CrossRef]
34. Nash, J.E.; Sutcliffe, J.V. River flow forecasting through conceptual models part I—A discussion of principles. *J. Hydrol.* **1970**, *10*, 282–290. [CrossRef]
35. Gupta, H.V.; Sorooshian, S.; Yapo, P.O. Status of Automatic Calibration for Hydrologic Models: Comparison With Multilevel Expert Calibration. *J. Hydrol. Eng.* **1999**, *4*, 135–143. [CrossRef]
36. Mann, H.B. Nonparametric Tests against Trend. *Econometrica* **1945**, *13*, 245–259. [CrossRef]
37. Kendall, M.G. *Rank Correlation Methods*; Griffin: Oxford, UK, 1948.
38. Gumus, V.; Avsaroglu, Y.; Simsek, O. Streamflow trends in the Tigris river basin using Mann−Kendall and innovative trend analysis methods. *J. Earth Syst. Sci.* **2022**, *131*, 34. [CrossRef]
39. Lian, Y.; Sun, M.; Wang, J.; Luan, Q.; Jiao, M.; Zhao, X.; Gao, X. Quantitative impacts of climate change and human activities on the runoff evolution process in the Yanhe River Basin. *Phys. Chem. Earth Parts A/B/C* **2021**, *122*, 102998. [CrossRef]
40. Immerzeel, W.W.; Pellicciotti, F.; Bierkens, M. Rising river flows throughout the twenty-first century in two Himalayan glacierized watersheds. *Nat. Geosci.* **2013**, *6*, 742–745. [CrossRef]
41. Chen, J.; Brissette, F.P.; Chaumont, D.; Braun, M. Performance and uncertainty evaluation of empirical downscaling methods in quantifying the climate change impacts on hydrology over two North American river basins. *J. Hydrol.* **2013**, *479*, 200–214. [CrossRef]
42. Chen, Q.; Chen, H.; Wang, J.; Zhao, Y.; Chen, J.; Xu, C. Impacts of Climate Change and Land-Use Change on Hydrological Extremes in the Jinsha River Basin. *Water* **2019**, *11*, 1398. [CrossRef]
43. Cui, H.; Jiang, S.; Gao, B.; Ren, L.; Xiao, W.; Wang, M.; Ren, M.; Xu, C.-Y. On method of regional non-stationary flood frequency analysis under the influence of large reservoir group and climate change. *J. Hydrol.* **2023**, *618*, 129255. [CrossRef]
44. Liu, X.; Yang, M.; Meng, X.; Wen, F.; Sun, G. Assessing the Impact of Reservoir Parameters on Runoff in the Yalong River Basin using the SWAT Model. *Water* **2019**, *11*, 643. [CrossRef]
45. Zhang, K.; Yuan, X.; Lu, Y.; Guo, Z.; Wang, J.; Luo, H. Quantifying the Impact of Cascade Reservoirs on Streamflow, Drought, and Flood in the Jinsha River Basin. *Sustainability* **2023**, *15*, 4989. [CrossRef]
46. Yun, X.; Tang, Q.; Wang, J.; Liu, X.; Zhang, Y.; Lu, H.; Wang, Y.; Zhang, L.; Chen, D. Impacts of climate change and reservoir operation on streamflow and flood characteristics in the Lancang-Mekong River Basin. *J. Hydrol.* **2020**, *590*, 125472. [CrossRef]
47. Zhang, P.; Cai, Y.; Xie, Y.; Yi, Y.; Yang, W.; Li, Z. Effects of a cascade reservoir system on runoff and sediment yields in a River Basin of southwestern China. *Ecol. Eng.* **2022**, *179*, 106616. [CrossRef]